MagnetoHydroDynamics Experiments with a Helical Channel in a 4T Superconducting Magnet

Ivan MONTERO[1], Alexandre ZAPATA[1], Yves DELANNOY[1], Nathanaël MACHICOANE[1]*

[1] Univ. Grenoble Alpes, CNRS, Grenoble INP, LEGI, 38000 Grenoble, France

[*] ivan-ernesto.montero-siles1@univ-grenoble-alpes.fr

Abstract: This paper details an experimental study of a magnetohydrodynamic (MHD) pump made of a helical channel inside a superconducting solenoidal magnet with a maximum intensity of 4 T, in conjunction with an electric field applied by platinum-coated titanium electrodes. This electric field is regulated by voltage (4-24 V) from a power supply which can provides up to 400 A. Experiments were conducted at various magnetic field intensities (3 T, 3.5 T, and 4 T at the center of the magnet) with different voltage levels and valve openings to examine the system's behaviour. Pressure sensors and flow rate measurements were taken to analyse the relationship between power supply, flow dynamics, and current limitations due to electrolysis-induced bubbles. These findings offer valuable insights for optimizing future MHD pumping systems.

Key words: MHD salt water, Pump MHD, Superconductor magnet.

1. Introduction. The experiments and result discussed herein were performed in order to conduct magnetohydrodynamic (MHD) pumping tests in a 4T magnetic field to prepare for a future phase of experiments at higher intensities of magnetic fields. These tests were conducted at the Néel Institute from January to February 2024, using a helical hydraulic channel with platinum-coated titanium electrodes placed in an existing superconducting magnet.

The magnet, provided by the Néel laboratory for the duration of the tests, contains a first-generation superconducting solenoid coil, cooled by helium and liquid nitrogen, and produces a magnetic field of 4 T at the center of the magnet (or less, depending on the coil's power supply). The tests were conducted with highly salted water (approximately 200 g/l) with a conductivity of 195 mS/cm (milli Siemens per centimeter).

The actual measurements presented in this paper will enable to calibrate the MHD models developed in the same project [1]. Additionally, the feedback presented in this paper aims at addressing future development and hydraulic design for the next experiences to come at higher intensities of magnetic field, such as 10 T.

2. Test Bench. The test bench designed for the MHD pump includes three main components: a 4T superconducting magnet, a tank with a helical channel and concentric electrodes, and an external hydraulic circuit. The superconducting magnet, cooled by liquid helium with an outer liquid nitrogen barrier, can generate a vertical magnetic field up to 4T at its center point. For magnetic fields up to 3.5T, a persistent mode can be used, while at 4T, the coil must remain connected to a power supply for better protection against quenching.

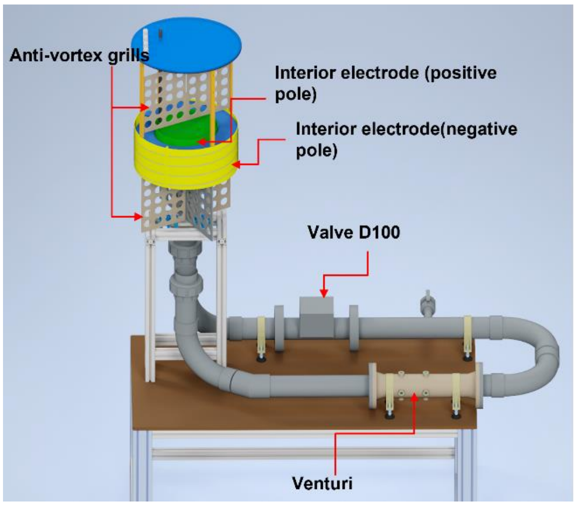

Figure 1. Detail of the helical channel and the electrodes inside the tank, the control valve, and the venturi for flow measurement.

The tank features anti-vortex grids to minimize tangential flow and includes a stainless-steel cooling tube immersed in the saltwater. The helical channel, placed between the anti-vortex grids, contains electrodes made of platinum-coated titanium for their resistance to corrosion and favorable electrochemical properties. The external hydraulic circuit includes a regulating valve to control the flow. This setup is crucial for different series of experiments with varying hydraulic resistance of the circuit. A configuration without valve was also used in order to evaluate the pump plugged to a circuit with minimum hydraulic resistance.

The helical channel is equipped with six pressure taps through the inner electrode, connected by flexible tubes through the bottom of the tank to pressure sensors, located 3.5m from the magnet axis to protect them from magnetic field influence. The pressure taps are spaced half a turn apart along the helical channel, with tap number 1 located a quarter turn from the inlet and tap 6 a quarter turn from the outlet. The pressure sensors measure absolute pressure up to 1600 mBar.

3. Experimental conditions. See Table 1

Table 1. **Test configurations**

Configuration	**Magnetic Field Intensity [T]**	**Control**
No valve "SV"	3, 3.5, and 4	Imposed voltage ramp 4-20V
Open valve "VO"	3, 3.5, and 4	Imposed voltage ramp 4-20V
Valve position 11 "V11" (60% flow)	3, 3.5, and 4	Imposed voltage ramp 4-20V
Variable valve	3, 3.5, and 4	Valve adjustment, voltage fixed at 10V then 15V

4. Findings

4.1 Pump equivalent performance. Magnetohydrodynamic (MHD) pumping is due to the interaction of the magnetic induction $\boldsymbol{B}$ with the current density $\boldsymbol{j}$ induced in the saltwater of electrical conductivity σ by applying an electric field $\boldsymbol{E}$ between the electrodes. When the water moves at velocity $\boldsymbol{U}$, the current density is given by Ohm's law [2]:

$$\boldsymbol{j} = \sigma(\boldsymbol{E} + \boldsymbol{U} \wedge \boldsymbol{B}) \Rightarrow j_r = \sigma(E_r - UB_z)$$

where $\boldsymbol{j_r}$ is the radial current density, $\boldsymbol{E_r}$ is the radial electric field component and $\boldsymbol{B_z}$ is the magnetic field component in the z direction; while $\boldsymbol{U}$ is the velocity of the water in the helical channel. The helical channel acts as a pump, providing hydraulic energy to the flow proportional to the product of the electrical current ($\boldsymbol{I}$) and the magnetic field ($\boldsymbol{B}$). This relationship is crucial as it primarily determines the integral of $\boldsymbol{j} \wedge \boldsymbol{B}$, with the magnetic field and current density distributions ($\boldsymbol{j}$) remaining largely constant.

By integrating over the entire volume traversed by the electric currents, we obtain the electric current ($\boldsymbol{I}$) that passes from one electrode to the other through the saltwater solution under the form, $I = (\Delta\varphi_{mhd} - cQB)/R$, where $\Delta\varphi_{mhd}$ is the voltage difference applied to the solution. $\Delta\varphi_{mhd}$ differs from the voltage applied by the electric supply to the electrodes because of the electrode potentials E_a and E_c (E_a>0 at the anode and E_c<0 at the cathode), which are necessary for the half-reactions of saltwater electrolysis. E_a and E_c represent the potential of each electrode relative to the solution in its vicinity, so the potential difference applied to the solution (excluding the thin electrochemical layers) is $\Delta\varphi_{mhd} = (\varphi_a - E_a) - (\varphi_c - E_c)$. Therefore, the voltage applied to the solution is equal to the voltage $\Delta\varphi_{el} = \varphi_a - \varphi_c$ applied to the electrodes minus an "electrochemical voltage loss" $\Delta\varphi_{ch} = E_a - E_c$, which tends towards a constant $\Delta\varphi_{ch0}$ at zero current and increases with current. Assuming, to the first order, that this increase occurs at a constant slope (i.e., $\frac{\mathrm{d}\Delta\varphi_{ch}}{dI} = C^{ste} = R_{ch}$), we have $\Delta\varphi_{el} = \Delta\varphi_{ch0} + (R + R_{ch})I + cQB$.

To highlight this behavior in our experiments, we adjusted the constants $\Delta\varphi_{ch0}$, $(R + R_{ch})$, and c of the above equation to best fit (in the least squares sense) the experimental results obtained at $\Delta\varphi_{el} \leq 14\ V$. Results at higher voltages are considered too disturbed by the presence of gas in the channel and therefore are not included in the analysis discussed herein, nevertheless we plotted them in **Figure 2** (points inside frames) with the points used for further analysis.

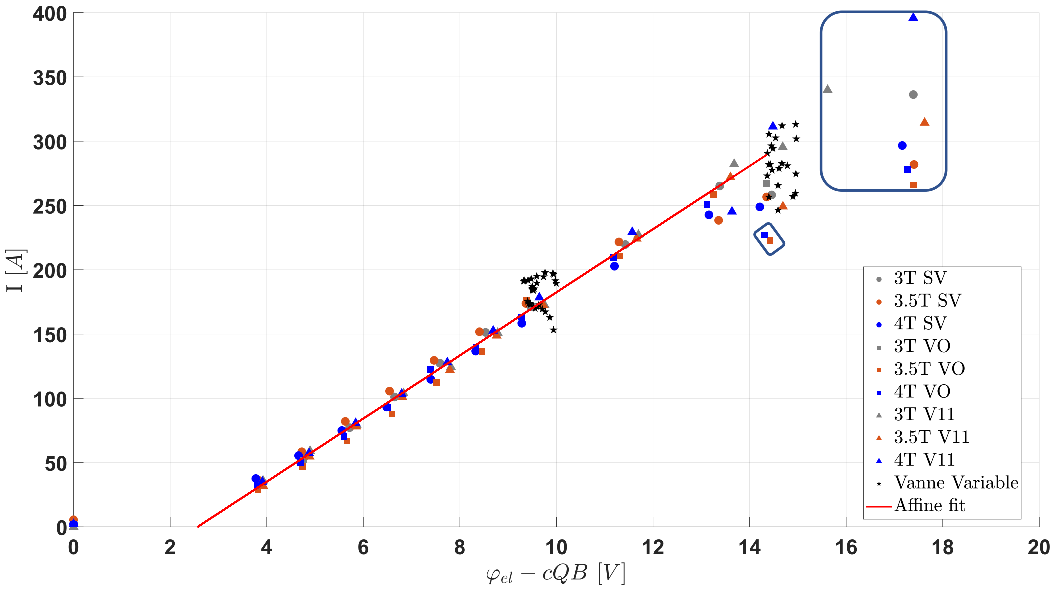

Figure 2. Current I as a function of the voltage at the electrodes, corrected for the $U \wedge B$ effect. The framed points, disturbed by the presence of gas in the channel are not used for the analysis.

4.1.1 Hydraulic Load and Pressure Gain In a constant cross-section pump, kinetic energy remains nearly constant along the helix, translating hydraulic head into pressure (Δp_{mhd}). This pressure gain corresponds to mechanical power supplied to the fluid ($P_{meca} = Q.\Delta p_{mhd}$), with some power lost by friction ($P_{hyd} = Q.\Delta p_{pompe} = P_{meca} - P_{loss}$).

4.1.2 Pressure Measurement Pressure was measured between points 1 and 6 (Δp_{61}) to avoid disturbances from the channel's ends. The pressure difference is expected to follow the relation: $\Delta p_{61} = a_{61}.I.B - K_{61}.Q^2$ where $K_{61}$is the hydraulic resistance (constant at high Reynolds numbers) [3], and $a_{61}$is a constant standing for the ratio of pressure gain in mbar achieved for each unit of $I{\cdot}B$ [A.T] applied [4, 5].

Experimental observations for different circuit resistances (VO, SV, V11) and for different magnetic fields (3 T, 3.5 T, 4 T) showed varying pressure gain in the helical channel, whereas without a magnetic field, the pressure loss in the helical channel has been measured with the help of an external pump. Data fitting of the MHD experiments provided the following coefficients:

$$a_{61} = 0.1457 \text{ mbar/A/T} = 14.57 \text{ m}^{-1}$$
$$K_{61} = 0.0273\text{mbar}/(\text{m}^3/\text{h})^2$$

The coefficient $a_{61}$is comparable to theoretical values for a straight channel. To visualizing the quality of this fit, we have plotted in **Figure 3**. $\Delta p_{mhd} = \Delta p_{61} + K_{61} Q^2$ versus IB, showing only minor deviations from the linear law $\Delta p_{mhd} = a_{61} IB$.

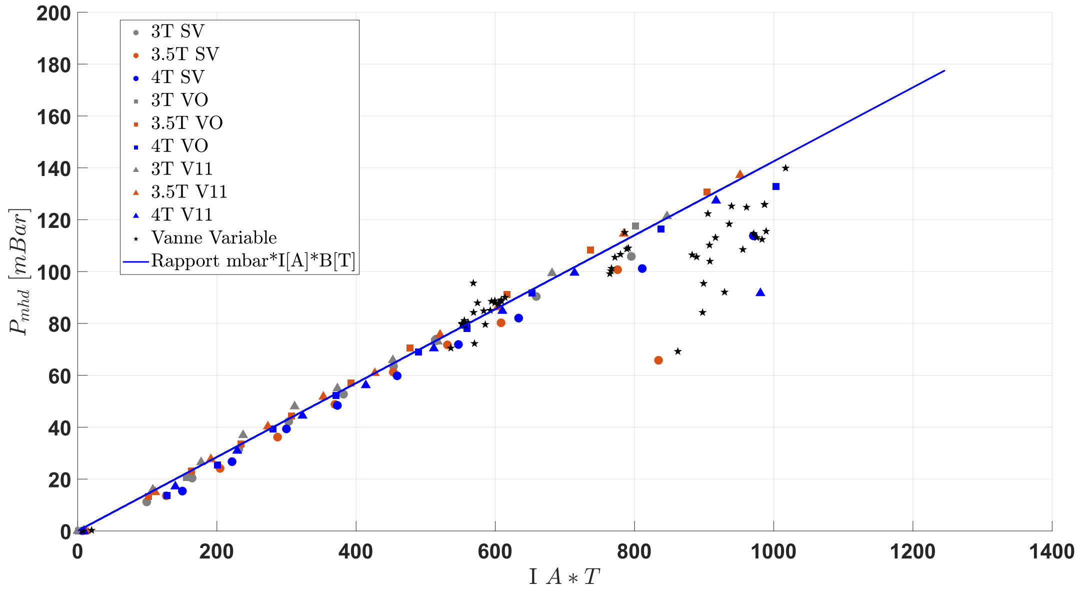

Figure 3. Pressure gain due to MHD effects vs. the driving term I*B.

Hydraulic resistance validation: comparing friction losses in MHD and non-MHD tests (**Figure 4**) showed differences below 0.5 mbar, suggesting that magnetic field effects on friction losses could not be conclusively evaluated with this setup. In that figure the hydraulic loss with magnetic field has been calculated by $\Delta p_{loss} = a_{61} IB - \Delta p_{61}$

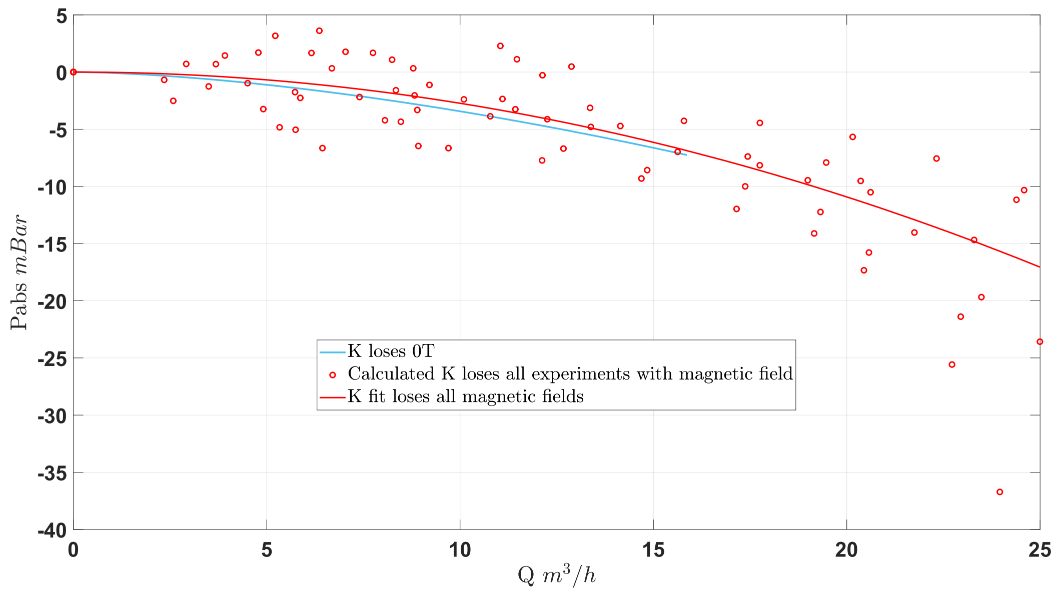

Figure 4. Pressure losses in the helical channel, "VO" tests with and without magnetic field.

4.2 Bubble generation and hydraulic performance impact Electrolysis during the experiments produced gases (chlorine or oxygen at the anode and hydrogen at the cathode), forming bubbles that impeded current flow if they accumulated near the electrodes. The solution became opaque with bubbles, within a minute of current application and cleared quickly once the current stopped.

At currents above 240A (14V), the bubble quantity significantly reduced hydraulic performance by decreasing solution conductivity. To counter this, the current was rapidly increased to the desired level, allowing a short window (about one minute) for normal operation before bubbles accumulated.

Experiments above 240A were mostly avoided due to excessive bubble generation. Estimates indicated about 5.31 liters of bubbles were generated at currents above 240A, calculated based on the observed level rise in the tank. Using Faraday's law [6], the volume of hydrogen and oxygen produced at 280A over 120 seconds was estimated at 6.28 liters (4.1 liters hydrogen, 2.18 liters oxygen).

4.3 Choosing the Best Insulating Paint Tests identified PVC glue as the most effective insulating paint for titanium electrodes, enduring over 96 hours in saline solution, whereas black anticorrosion paint eventually failed. Despite a layered combination of PVC glue and black paint, the PVC coating deteriorated on platinum-coated surfaces and on overheated titanium bars, indicating a need to explore alternative materials for extreme conditions like chlorine exposure.

5. Conclusions

Among the most notable findings was the impact of bubbles on hydraulic and electrical performance for high current experiments (above 240A), where excessive bubble formation reduced the apparent conductivity. Despite this limitation in current we successfully managed to characterize the behavior of the MHD pump in our test bench. This behavior is described by two characteristic laws (electrical and hydraulic) with coefficients mentioned in this paper.

Concerting the titanium coating, PVC glue was found effective for insulating titanium but degraded over time, especially under high temperatures and when applied on a platinum coating.

Future improvements will focus on thermal management, reduction of bubble effects, and finding more resilient protective materials for the electrodes' surfaces.

REFERENCES

[1] A. ZAPATA ET AL., CFD simulation of helicoidal magnetohydrodynamic pump in closed circuit. *13th PAMIR International Conference*, Carry le Rouet, France, (2024).

[2] J.P. THIBAULT, Propulsion MagnétoHydroDynamique (MHD) en eau de mer. *La Revue 3EI*, p. 31, (2018).

[3] I. E. IDELCHIK, *Handbook of Hydraulic Resistance*, New York: Begell House (2021).

[4] B. ZHAO ET AL., Experimental Study on Superconducting Helical Channel MHD Thruster, *42nd AIAA Plasmadynamics and Lasers Conference*, Honolulu, Hawai (2011)

[5] Y. PENG ET AL., Performance Analyses of Helical MHD Thruster in 14 Tesla, *33rd AIAA Plasmadynamics and Lasers Conference*, Maui, Hawai (2002)

[6] P BOISSONNEAU, J-P THIBAULT, Experimental analysis of couplings between electrolysis and hydrodynamics in the context of MHD in seawater J. Phys. D: Appl. Phys. vol 32 (1999).